International Journal of GEOMATE, Nov, 2022, Vol.23, Issue 99, pp.1-8
ISSN: 2186-2982 (P), 2186-2990 (O), Japan, DOI: https://doi.org/10.21660/2022.99.3640
Geotechnique, Construction Materials and Environment

EFFECT OF FIBERS ON THE COMPRESSIVE AND TENSILE STRENGTHS OF SAND CONSIDERING FAILURE MODE

*Jakhongirbek Ganiev[1], Masaki Nakano [2] and Takayuki Sakai[3]

[1,2,3]Department of Civil Engineering, Nagoya University, Japan

*Corresponding Author, Received: 12 Oct. 2022, Revised: 30 Oct. 2022, Accepted: 16 Nov. 2022

ABSTRACT: In geotechnical engineering, fiber reinforcement for improving the stability and strength of soils is of considerable interest. According to previous studies, fibers enhance compressive strength significantly, whereas the contribution of fibers in extension is limited. However, this phenomenon has not been analyzed comprehensively. Therefore, conventional triaxial compression and extension tests were conducted under both drained and undrained conditions on fiber-reinforced sand specimens to elucidate the influence of fibers on tensile strength. The compression behavior was significantly influenced by the presence of fibers and confining pressure, independent of the drainage conditions. However, in the extension experiments, the properties of the fiber-reinforced sand under drained conditions differed from those of unreinforced specimens. The tensile strength of the fiber-reinforced sand was relatively enhanced under undrained conditions. Both unreinforced and fiber-reinforced sands experienced deformation throughout the entire height of the specimen, and their central regions bulged under loading conditions. With an increase in confining pressure under unloading conditions, the unreinforced sand specimen developed a double "necking" shear band in the center with more pronounced strain localization. In contrast, the failure modes of fiber-reinforced sand in drained conditions were characterized by strain localization and shear bands transferred to the bottom part of specimens. According to the experimental results and their repeatability, a conventional triaxial extension test may be insufficient to evaluate tensile strength accurately. In addition, a possible explanation for the fiber-sand interaction mechanism has been proposed based on the obtained results and failure mode analysis.

Keywords: Sand, Fiber, Triaxial Compression, Triaxial Extension, Failure mode

1. INTRODUCTION

Reinforcement of soils using natural or synthetic fibers is an alternative solution for improving the stability of earth-retaining structures, particularly for slopes, dams, and embankments. The effectiveness of fiber reinforcement depends on both soil (shape and size of particles, gradation, density, and composition) and fiber parameters (type, shape, aspect ratio, elasticity modulus, and tensile strength). In addition, the distribution and orientation of fibers after sample preparation also affect the effectiveness of fiber reinforcement. The effect of short flexible fibers on the compressive strength of soils has been demonstrated by numerous studies [1-10] through various experimental programs, including direct and ring shear tests and consolidated drained and undrained triaxial tests. Most previous studies reported that the fibers affected the compressive strength considerably.

Several attempts have been made to add fibers as a reinforcing material to the soil for increasing the tensile strength of the composite [11-14]. However, according to previous studies, the addition of fibers has a negligible effect on increasing the tensile strength of soils. Through drained triaxial extension experiments, some studies revealed that fibers are ineffective as reinforcing materials; the behaviors of unreinforced and fiber-reinforced specimens with different relative densities and sheared under various stresses exhibited insignificant differences [6] [11] [16]. Ibraim et al. [12] showed that, in undrained conditions, the tensile strength of sandy soil increased slightly with increasing fiber content, whereas Chen [11] did not observe similar behavior in fiber-reinforced silty sand soil, despite shearing the soil under different stresses. Interestingly, drained triaxial extension tests conducted by Palacios et al. [16] revealed that the tensile strength of fiber-reinforced sand was lower than that of unreinforced sand samples.

A possible cause behind the inefficiency of fiber reinforcement in increasing the tensile strength is the deformation shape of the specimen, which affects both compressive and extensive strengths. Few studies have investigated the failure modes of fiber-reinforced samples. Chen [11] found that fibers had no influence on the failure modes of specimens with identical deformation shapes at the end of the triaxial extension tests (ε_q=25%). Deformations such as "necking" and shear banding under strain localization were

observed in the central sections of both unreinforced and fiber-reinforced specimens. In [15], torsional shear tests were conducted under various principal stress directions. This study also found that the failure modes of sandy specimens were unaffected by the presence of fibers and that the orientation of the shear bands in the fiber-reinforced sand was similar to that in the unreinforced sand. Few studies have investigated the effect of fiber reinforcement by considering the difference in the failure modes and an unidentified dependency exists between the reinforcing effect of fibers and failure modes.

2. RESEARCH SIGNIFICANCE

This study investigated the effect of fiber reinforcement on the compressive and tensile strengths of sand under various applied stresses, initial densities, and drainage conditions. We compared the tensile strength of sand, which is unaffected by the fibers, with its compressive strength in drained conditions. Studies concerning the effect of fibers on the failure modes and the correlation of soil strength with deformation shape are limited. Therefore, a possible dependency of soil strength on failure modes was analyzed with an emphasis on strain localization based on the drainage conditions. In addition, some limitations of current practices for extension experiments were explored.

3. MATERIAL AND METHODS

In all experiments, two materials were utilized: sandy soil as a host soil and a short discrete synthetic fiber as a reinforcing element.

3.1 Sand and Fiber

Standard Toyoura sand was used for all the experiments. Its grain size distribution is shown in Fig. 1. The Toyoura sand specific gravity (G_s) of 2.646. Its maximum and minimum void ratios (e_{max} and e_{min}) were 0.985 and 0.639, respectively.

Polyvinyl alcohol (PVA) fibers with a length of 12 mm and diameter of 0.04 mm were used as the reinforcing material (Fig. 2). The fibers had a specific gravity (G_f) of 1.3, tensile strength (τ) of 1560 MPa, and elastic modulus (E) of 41 GPa.

The fiber content $\boldsymbol{w_f}$ is defined by the mass ratio.

$$\boldsymbol{w_f} = \frac{\boldsymbol{m_f}}{\boldsymbol{m_{sp}}}, \quad (1)$$

where m_f and m_{sp} are the masses of the fibers and sand particles, respectively.

In this study, three different fiber contents, 0.0%, 0.2%, and 0.4%, were adopted to obtain the correlation of fiber reinforcement to soil strengths in both the compression and extension experiments.

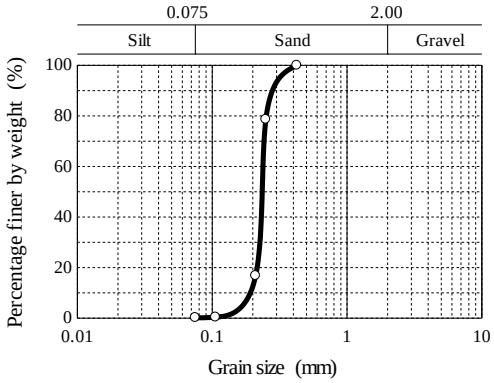

Fig. 1 Cumulative grain size distribution of Toyoura sand (Ganiev et al. [10])

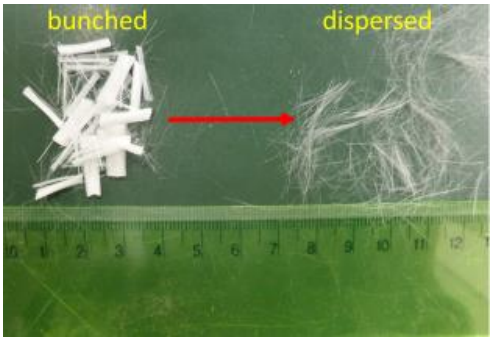

Fig. 2 PVA fibers in initial and pre-mixing condition

3.2 Sample Preparation

The specimen preparation involved mixing the fibers with sand and molding. The samples were prepared through a trial-and-error method in four different ways [10]. The optimum approach was to mix the sand and fibers manually in dry conditions and compact the composite mass through vibration. First, the fibers were weighed to obtain the desired percentage of fibers. The fibers had to be dispersed from their bunched state before adding them to the sand, as shown in Fig. 2. Next, a small number of fibers was placed on the plate and covered with a layer of sand. This action was repeated until all fibers and sand were added and resembled a "sandwich." Manual mixing using a scoop was sufficient to homogenize the materials for low percentages of added fibers (0.2% and 0.4%).

The masses were molded once the fiber–sand mixture appeared to be visually uniform. A cylindrical specimen having a height of 100 mm and diameter of 50 mm was used, and an initial

relative density D_r was established. All samples were compacted into one layer to investigate the effect of the random orientation of the fibers. Both unreinforced and fiber-reinforced sand was compacted by side tapping and vibration.

Additionally, the exhumed samples were analyzed to ensure the homogeneity of the samples and the equal distribution of fibers across the entire height of the specimen and to prevent localizations in the bottom or top parts (Fig. 3). An exhumed sample was divided into four equal parts (B1, B2, T1, and T2), and the ingredients were separated and weighed (a specimen having a fiber content 0.4% and with D_r = 60% is shown in Fig.3). Maximum amount of fibers were separated from the sand by sieving the mixture several times using sieves of sizes of 420 μm and 360 μm. The fibers thus separated were then weighed. The total initial weight of the fibers, $m_{f,t}$, was 1.17 g. The weight of separated fibers, $m_{f,s}$, was 1.09 g. After obtaining the weight of each part, the sand particles were sieved again, and an additional 0.05 g of fibers ($m_{f,a}$) was separated. Therefore, the total weight of fibers separated from the sand was $m_{f,t} = m_{f,s} + m_{f,a}$ = 1.09 + 0.05 = 1.14 g. As can be observed from Fig. 3, the fibers were uniformly distributed in each part.

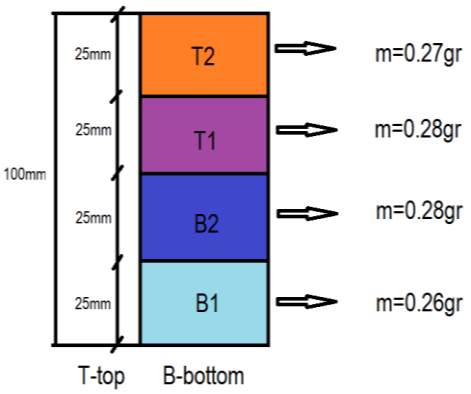

Fig. 3 Exhumed and dried sand samples with 0.4% fiber content

After placement, the specimen was saturated. First, CO_2 was infiltrated into the specimen to replace the air in the pores. Then, the specimen was saturated with de-aired water, expelling the CO_2 as completely as possible. The values of Skempton's coefficient B for all specimens exceeded 0.95. Next, the specimens were consolidated. All specimens were sheared at a strain rate of 0.5%/mm until the axial strain exceeded 20% in compression and 15% in extension. The experiments conducted are listed in Table 2.

4. RESULTS AND DISCUSSION

Consolidated drained (*CD*) and undrained ($\overline{CU}$) triaxial compression and extension tests were conducted on unreinforced sand and sand reinforced with fiber contents of 0.2% and 0.4%. All the specimens were consolidated isotropically and sheared under two different confining pressures: 100 kPa and 200 kPa. To analyze the effect of the confining pressure explicitly, a higher confining pressure of 300 kPa was applied during the drained extension experiments.

Table 2 List of experiments

Test	w_f, %	Type	p'_0, kPa	e_0	D_r
Consolidated drained triaxial experiments					
C-100-00	0.0	C	100	0.705	80
C-100-02	0.2	C	100	0.702	80
C-100-04	0.4	C	100	0.700	80
C-200-00	0.0	C	200	0.703	80
C-200-02	0.2	C	200	0.700	80
C-200-04	0.4	C	200	0.698	80
E-100-00	0.0	E	100	0.707	80
E-100-02	0.2	E	100	0.705	80
E-100-04	0.4	E	100	0.704	80
E-300-00	0.0	E	300	0.704	80
E-300-02	0.2	E	300	0.702	80
E-300-04	0.4	E	300	0.701	80
Consolidated undrained triaxial experiments					
C-100-00	0.0	C	100	0.844	40
C-100-02	0.2	C	100	0.827	40
C-100-04	0.4	C	100	0.835	40
C-200-00	0.0	C	200	0.840	40
C-200-02	0.2	C	200	0.827	40
C-200-04	0.4	C	200	0.826	40
E-100-00	0.0	E	100	0.838	40
E-100-02	0.2	E	100	0.837	40
E-100-04	0.4	E	100	0.840	40
E-200-00	0.0	E	200	0.838	40
E-200-02	0.2	E	200	0.837	40
E-200-04	0.4	E	200	0.840	40

C-COMPRESSION; E-EXTENSION

4.1 Drained Shear Behavior in Triaxial Compression and Extension Experiments

Figure 4 shows the results of the consolidated drained triaxial compression tests on both the unreinforced and 0.2% and 0.4% fiber-reinforced sands under confining pressures of 100 kPa and 200 kPa. All experiments were performed three times to confirm the repeatability of the mechanical behaviors and to ensure the homogeneity of the fiber distribution by comparing the deformation shapes of the specimens. Figure 4 shows the variation of deviator stress q with axial strain ε_a and the dependency of volumetric strain ε_v on ε_a. The latter describes the dilatancy behavior.

The residual stress in the unreinforced sand under the confining pressure of 100 kPa was 250 kPa, while the residual stresses in the specimens reinforced with 0.2% and 0.4% fiber contents were 320 kPa and 390 kPa, respectively (Fig. 4a). The values of the deviator stress of the specimens

reinforced with 0.2% and 0.4% fibers at the end of shearing were 28% and 56% higher than that of the unreinforced specimen, respectively. As evident from the $\varepsilon_v - \varepsilon_a$ curve, the fiber-reinforced specimen experienced lower volumetric expansion. Furthermore, the higher the fiber content, the lesser the volumetric expansion, that is, the fibers contracted the sandy specimen.

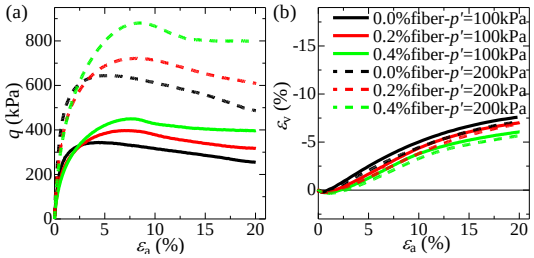

Fig. 4 Drained triaxial compression test results performed under confining pressures of 100 kPa and 200 kPa

Increasing the confining pressure increased the deviator stresses and decreased the volumetric expansion in both the unreinforced and fiber-reinforced specimens. In particular, at a confining pressure of 200 kPa, the deviator stresses in the specimens reinforced with 0.2% and 0.4% fibers were 127% and 160% higher than that in the unreinforced sand at 20% axial strain. The volumetric expansion of the fiber-reinforced specimens was lower than that of the non-reinforced sand specimens.

In compression tests, the mechanical behaviors of both the unreinforced and fiber-reinforced specimens can be obtained with good repeatability. According to these results, the compression behavior is significantly influenced by the fiber content. The effect of increasing the confining pressure was observed in both stress-strain curves and dilatancy behaviors, which showed an increase in the maximum and residual deviator stresses and a decrease in the volumetric expansion, respectively.

Figure 5 shows the results of drained triaxial extension tests conducted under confining pressures of 100 kPa and 300 kPa on the unreinforced and 0.2% and 0.4% fiber-reinforced specimens. Unlike the compression behavior, which was influenced by both fiber content and confining pressure, the tensile strength of the fiber-reinforced specimens was not influenced by the presence of fibers. The shearing behavior of fiber-reinforced sands under the confining pressure of 100 kPa revealed that the inclusion of fibers had a negligible effect: the stress-strain and volumetric change curves of unreinforced and reinforced specimens exhibited similar behaviors. The peak and post-peak deviator stresses of all specimens increased as the confining pressure increased to 300 kPa. The tensile strength increased only because of the higher confining pressure; the fibers did not contribute to the increase in tensile strength. The volumetric change decreased as the confining pressure increased. In other words, the higher the confining pressure, the lower the volumetric expansion, which was similar to the behavior observed in the compression experiments.

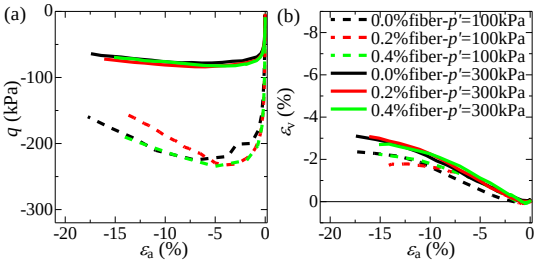

Fig. 5 Drained triaxial extension test results performed under confining pressures of 100 kPa and 300 kPa

4.2 Undrained Shear Behavior in Triaxial Compression and Extension Experiments

Figure 6 and Figure 7 present the results of consolidated undrained triaxial compression experiments conducted under confining pressures of 100 kPa and 200 kPa, respectively. The specimens were placed in medium-dense condition and sheared**.**

The behavior of the specimen having a fiber content of 0.4% was similar to that of loose sand; compared to other specimens, it showed a greater reduction in the initial stiffness (q– ε_a curves), the larger initial decrease in the mean effective stress, and higher positive pore water pressure (PWP) at smaller strains. However, the deviator stresses of the fiber-reinforced sand specimens increased with shear progression. The deviator stresses of the 0.2% and 0.4% fiber-reinforced sand specimens became higher than that of the unreinforced sand under both confining pressures. The greater initial reduction in deviator stresses and the more pronounced softening behavior in the fiber-reinforced specimens were attributed to the anisotropic effect [17]. In addition, after reaching the phase transformation point, the stress ratios of the 0.2% and 0.4% fiber-reinforced sand specimens became higher than that of the unreinforced specimen with shear progression. PWP generation was similar to the behavior of volumetric change in unreinforced and fiber-reinforced sand under drained conditions, wherein fiber-reinforced specimens contracted more and exhibited a smaller dilatancy ratio than the unreinforced specimens.

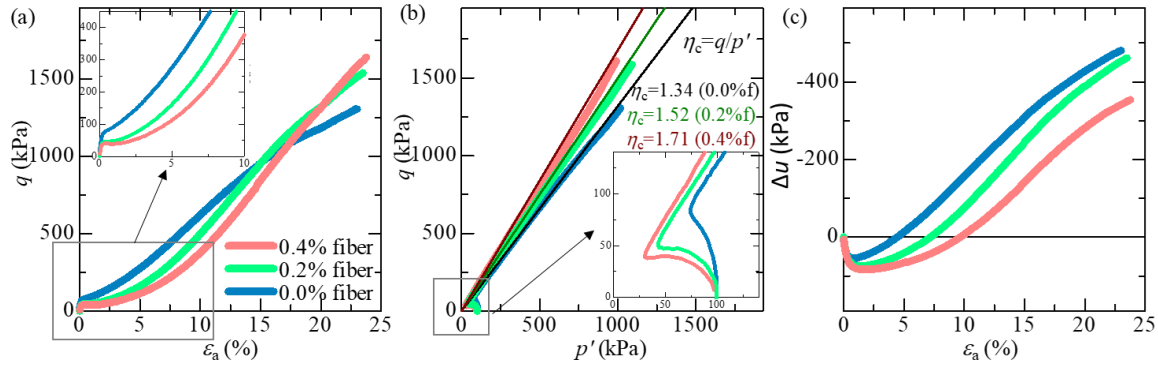

Fig. 6 Undrained triaxial compression test results performed under 100 kPa confining pressure

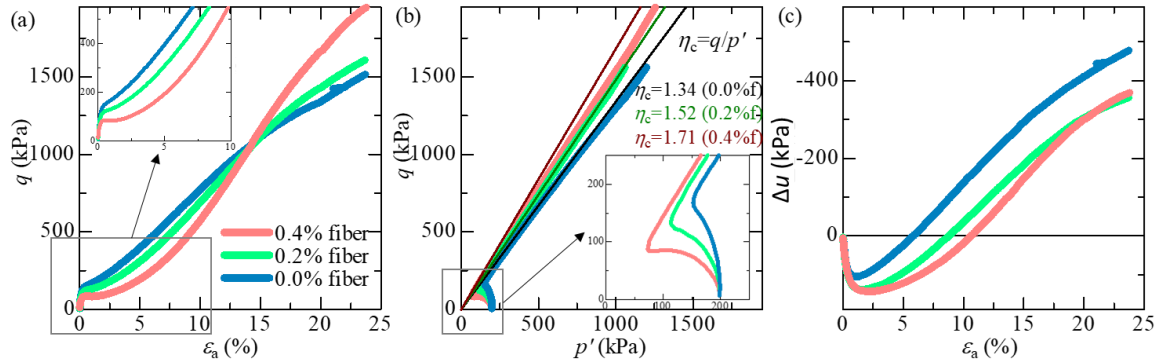

Fig. 7 Undrained triaxial compression test results performed under 200 kPa confining pressure

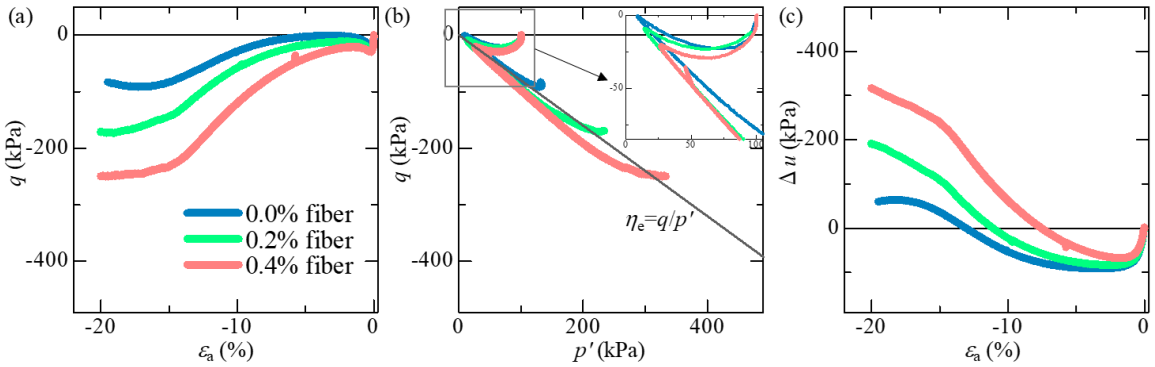

Fig. 8 Undrained triaxial extension test results performed under 100 kPa confining pressure

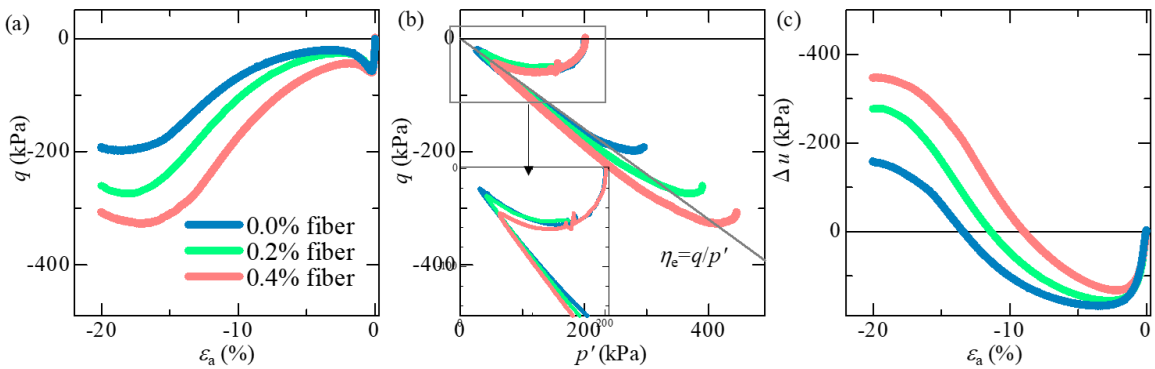

Fig. 9 Undrained triaxial extension test results performed under 200 kPa confining pressure

Figure 8 and Figure 9 present the results of consolidated undrained triaxial extension experiments conducted under confining pressures of 100 kPa and 200 kPa, respectively, on unreinforced and fiber-reinforced specimens. Unlike the drained behavior of unreinforced and fiber-reinforced sand under extension, the undrained tensile strength of sand was affected by fiber inclusion. Particularly, the tensile strength ($q - \varepsilon_a$ curves) of sand increased with the increase in fiber content under both confining pressures. Furthermore, the deviator stresses increased with the increase in confining pressure.

The fiber-reinforced sand specimens exhibited a less decrease in the effective stress with strain (strain-softening) and a higher stress ratio up to a point, after which all specimens experienced a reduction in deviator stress. The effective stress path thus formed a "hook." The formation of the "hook" in both unreinforced and fiber-reinforced grains of sand was attributed to strain localization and discernible shear banding, after which the shear behavior could not be considered as a one-element behavior. The effect of strain localization is discussed in the next section. The unreinforced sand initially experienced a higher positive PWP compared to the fiber-reinforced sands, and the excess PWP was reduced in the end. Furthermore, the PWP values changed from positive to negative at higher axial strains as confining pressure increased. In particular, the higher the confining pressure, the higher the initial PWP and the higher the negative PWP at the end of the test. The tendency to generate a higher negative PWP in fiber-reinforced sands might be a possible effect of increasing the tensile strength in contrast to the drained condition: no difference was observed between the behaviors of volumetric change in unreinforced and fiber-reinforced sands during the drained extension tests.

4.3 Discussion Based on Failure Mode Analysis Under Loading and Unloading Conditions

The mechanism of fiber reinforcement involves a complicated interaction between sand particles and fibers. The addition of fibers improved the compressive strength of the specimens effectively in both drained and undrained conditions, whereas the fibers improved the tensile strength of the specimens only in the undrained condition. To investigate the various aspects and factors related to the effects of the fiber reinforcement, a macro mechanical analysis was performed through failure mode analysis.

Figures 10–13 illustrate the failure modes of the unreinforced and fiber-reinforced specimens at 20% axial strain in triaxial compression tests and at 15% axial strain in triaxial extension tests under drained conditions and two different confining pressures. Notably, shear bands started forming in the unreinforced sand and fiber-reinforced sands at smaller axial strains. The given failure modes were the only reference to the fully formed shear bands at the end of the tests.

The failure modes of the unreinforced and 0.2% and 0.4% fiber-reinforced sand specimens in the compression tests were identical under the two confining pressures (Figs. 10–11). Deformation occurred throughout the height of the specimens, and the centers of the specimens bulged. The number of shear bands was higher in the specimens with higher fiber content and increased under higher confining pressures, which was accompanied by strain localizations that were more apparent. Unlike the deformation shapes observed in the compression test, the deformation shapes of the fiber-reinforced specimens in the triaxial extension tests were different from those of the unreinforced sand. The unreinforced samples exhibited a "necking" in the center (Fig. 12a), and the shear bands became more predominant under a higher confining pressure, which was accompanied by evident double necking (Fig. 13a). In contrast, the shear bands in the fiber-reinforced sand were observed at the bottom and the upper part of the sample was un-deformed. Under a lower confining pressure, no sharp strain localization was observed, whereas strain localization and explicit shear band formation occurred under the highest applied confining pressure of 300 kPa.

The negligible effect of fibers in increasing the tensile strength of sand under drained conditions may be explained by the "transfer" of shear bands to the bottom in the reinforced specimens. To explore this, the failure modes under undrained conditions were analyzed. Figures 14–17 illustrate a series of failure modes developed under the undrained condition in compression and extension tests. The failure modes of unreinforced and fiber-reinforced sands observed in the undrained triaxial compression test were identical, similarly to the failure modes under the drained condition (Figs. 14–15). The deformation in both the unreinforced and fiber-reinforced sand specimens occurred throughout the entire height and the centers of the samples bulged. The deformation shapes under compression in drained and undrained conditions and the high reproducibility of the test results corroborate that the uniformity of the fiber distribution was relatively high. Furthermore, in the undrained extension experiments, the failure modes of the fiber-reinforced sand specimens were similar to those of the unreinforced specimens. In particular, deformation occurred approximately in the

centers in both the unreinforced and fiber-reinforced specimens; the shear bands formed were also similar. The enhancement of the tensile strength of sand with an increase in fiber content was observed in undrained triaxial extension experiments.

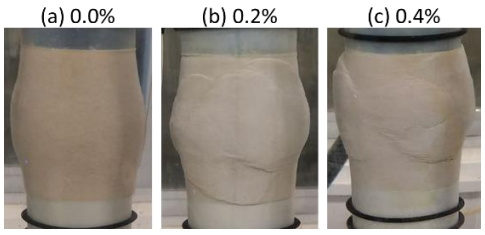

Fig. 10 Failure modes in *CD* compression sheared under a confining pressure of 100 kPa

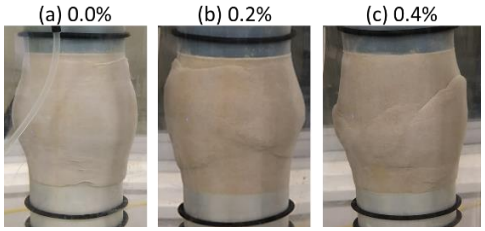

Fig. 11 Failure modes in *CD* compression sheared under a confining pressure of 200 kPa

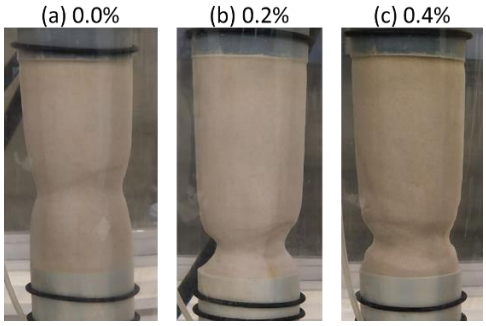

Fig. 12 Failure modes in *CD* extension sheared under a confining pressure of 100 kPa

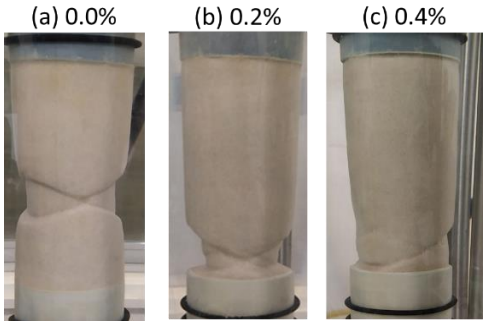

Fig. 13 Failure modes in *CD* extension sheared under a confining pressure of 300 kPa

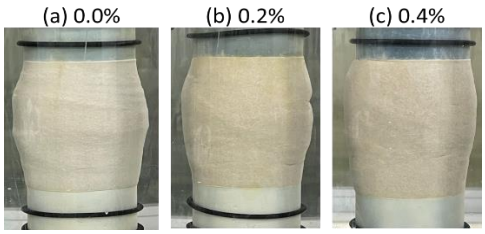

Fig. 14 Failure modes in $\overline{CU}$ compression sheared under 100 kPa confining pressure

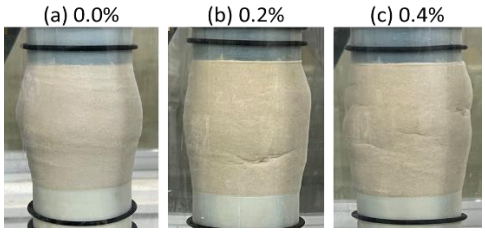

Fig. 15 Failure modes in $\overline{CU}$ compression sheared under 200 kPa confining pressure

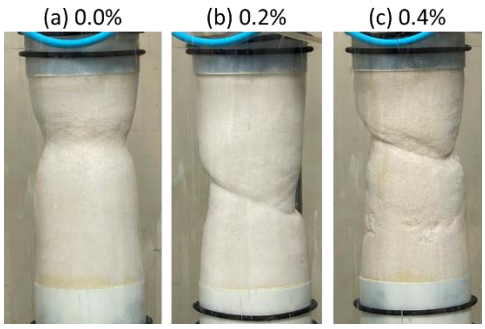

Fig. 16 Failure modes in $\overline{CU}$ extension sheared under 100 kPa confining pressure

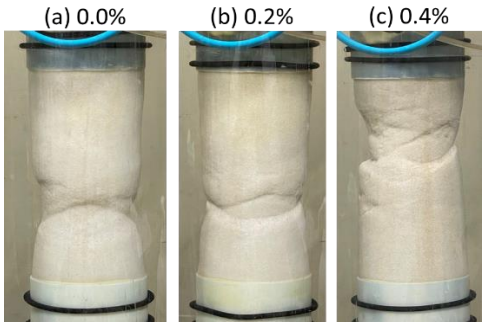

Fig. 17 Failure modes in $\overline{CU}$ extension sheared under 200 kPa confining pressure

Based on the mechanical behaviors of unreinforced and fiber-reinforced sands observed from the experiments and the deformation characteristics in drained and undrained conditions, the negligible effect of fiber in the drained extension experiment can be attributed to

the shear band transferred to the bottom of the specimens. This implies that the conventional triaxial apparatus may not be suitable for evaluating the tensile strength of fiber-reinforced sands precisely.

5. CONCLUSIONS

In this study, consolidated drained and undrained triaxial experiments were conducted at two different confining pressures. From the experimental results and discussion, the following conclusions can be drawn.

- The compression behavior was significantly influenced by the fiber content and confining pressure under both drained and undrained conditions. In contrast, in the extension tests, the effectiveness of fiber reinforcement was only observed under the undrained condition: under the drained condition, the shear behavior of sand was unaffected by the fiber content.
- The limited effect of fibers on enhancing the tensile strength may be attributed to the failure mode of the specimen. In *CD* extension tests, the unreinforced sample exhibited doubled "necking" shear bands in the central regions. In contrast, the reinforced specimens experienced transferred shear bands with strain localization at the bottom regions. However, in the *CD* and $\overline{CU}$ compression tests, both the unreinforced and fiber-reinforced specimens were entirely deformed with their centers bulged. According to the experimental results and failure mode analysis, conventional triaxial extension tests may be insufficient to evaluate the tensile strength of fiber-reinforced soils.

6. REFERENCES

[1] Ajayi O., Le Pen L., Zervos A. and Powrie, W., A behavioural framework for fiber-reinforced gravel, Géotechnique, Vol. 67, No. 1, 2017, pp. 56-68.

[2] Li H., Senetakis K. and Coop M.R., Medium-strain dynamic behavior of fiber-reinforced sand subjected to stress anisotropy, Soil Dyn. Earthq. Eng., Vol. 126, 2019, 105764.

[3] Gao Z. W., Lu D. and Huang M., Effective skeleton stress and void ratio for constitutive modeling of fiber-reinforced sand, Acta Geotech., Vol. 15, 2020, pp. 2797-2811.

[4] Heineck C.S., Coop M.R. and Consoli N.C., Effect of micro reinforcement of soils from very small to large shear strains, J. Geotech. Geoenviron. Eng., Vol. 131, No. 8, 2005, pp. 1024-1033.

[5] Ibraim E. and Fourmont S., Behaviour of sand reinforced with fibres, Soil stress-strain behaviour: measurement, Modelling, and Analysis, Ling, Callisto, Leshchinsky, Koseki (Eds.), Springer, 2007, pp. 807–918.

[6] Diambra A., Ibraim E., Muir Wood D., and Russell A.R., Fibre reinforced sands: experiments and modeling, Geotext. Geomembr., Vol. 28, 2010, pp. 238-250.

[7] Gao Z. and Huang M., Effect of sample preparation on the mechanical behavior of fiber-reinforced sand, Comput. Geotech. Vol. 133, 2021, 104007.

[8] Shukla S.K., Fundamentals of fibre-reinforced soil engineering, Singapore, Springer, 2017.

[9] Diambra A. and Ibraim E., Fibre-reinforced sand: interaction at the fibre and grain scale, Géotechnique, Vol. 65, No. 4, 2015, pp. 296–308.

[10] Ganiev J., Yamada S., Nakano M. and Sakai T., Effect of fiber-reinforcement on the mechanical behavior of sand approaching the critical state, J. Rock Mech. Geotech. Eng., Vol. 14, No. 4, 2022, pp. 1241-1252.

[11] Chen C., Triaxial compression and extension tests for fiber-reinforced silty sand, In GeoShanghai International Conference 2010 on Ground Improvement and Geosynthetics, 2010, pp. 367-376.

[12] Ibraim E., Diambra A., Muir Wood D. and Russell A.R., Static liquefaction of fibre reinforced sand under monotonic loading, Geotext. Geomembr., Vol. 28, 2010, pp. 374-385.

[13] Li J., Tang C., Wang D., Pei X. and Shi B., Effect of discrete fibre reinforcement on soil tensile strength, J. Rock Mech. Geotech. Eng., Vol. 6, 2014, pp. 133-137.

[14] Tang C., Shi B., Cui Y. and Wang D., Tensile Strength of Fiber-Reinforced Soil, J. Mater. Civ. Eng., Vol. 28, No. 7, 2016, 04016031.

[15] Mandolini A., Diambra A. and Ibraim E., Strength anisotropy of fiber-reinforced sands under multiaxial loading, Géotechnique, Vol. 69, No. 3, 2019, pp. 203-216.

[16] Palacios M., Casagrande M. and Consoli N., Behavior of a polypropylene reinforced sand under triaxial extension tests, Rio de Janeiro, MSc. Dissertation – Civil Engineering Department, Pontifical Catholic University of Rio de Janeiro, 2012.

[17] Ganiev J., Nakano M., and Sakai T., Numerical analysis of drained compression behavior of fiber-reinforced sand based on a soil skeleton structure concept, Comput. Geotech., Vol. 148, 2022, 104789.